



---

**Low Field Electrocaloric Effect at Isotropic - Ferroelectric Nematic Liquid Transition**

Journal:	<i>Soft Matter</i>
Manuscript ID	SM-ART-08-2024-000979.R2
Article Type:	Paper
Date Submitted by the Author:	09-Dec-2024
Complete List of Authors:	Adaka, Alex; Kent State University, Liquid Crystal Guragain, Parikshit; Kent State University College of Arts and Sciences, Perera, Kelum; Kent State University Nepal, Pawan; Kent State University, Department of Chemistry and Biochemistry Twieg, Robert; Kent State University, Department of Chemistry Jakli, Antal; Kent State University, Liquid Crystal

# Low Field Electrocaloric Effect at Isotropic - Ferroelectric Nematic Liquid Transition

A. Adaka<sup>1,2</sup>, P. Guragain<sup>4</sup>, K. Perera<sup>1,3</sup>, P. Nepal<sup>4</sup>, R. J. Twieg<sup>4</sup>, A. Jákli<sup>1,2,3</sup>

<sup>1</sup>Advanced Materials and Liquid Crystal Institute, Kent State University, Kent OH, 44242, USA

<sup>2</sup>Materials Science Graduate Program, Kent State University, Kent OH, 44242, USA

<sup>3</sup>Department of Physics, Kent State University, Kent OH, 44242, USA

<sup>4</sup>Department of Chemistry and Biochemistry, Kent State University, Kent, OH 44242, USA

## Abstract

*The study of electrocaloric effects (ECE) in solid state materials such as ferroelectric ceramics and ferroelectric polymers have great impact in developing cooling systems. Here we describe ECE of a newly synthesized ferroelectric nematic liquid crystal compound at the isotropic ferroelectric nematic ( $I-N_F$ ) phase transition. While for DC field the Joule heat completely suppresses the ECE,  $E \leq 1.2 \text{ V}/\mu\text{m}$ ,  $f \geq 40 \text{ Hz}$  fields increase optical transmittance, which by comparison with a zero-field transmittance versus temperature plot, means a shift of transition temperature. It implies that one can drive the phase transition of interest using an electric field, via ECE with  $\sim 1.7 \times 10^{-6} \text{ Km/V}$  EC responsivity. Importantly, the required field is two orders of magnitude smaller than typical for other EC materials. An EC effect under such low fields is a unique property of ferroelectric nematic liquid crystals. The specific EC energy can be increased considerably by reducing the ionic content, thus suppressing the Joule heat.*

**Keywords:** Liquid crystal, electrocaloric effect, transition temperature change liquid crystal, direct isotropic to ferroelectric nematic.

## I. Introduction

Over the years there have been significant improvement in various caloric effects such as mechanocaloric (barocaloric and elastocaloric), magnetocaloric and electrocaloric effects for important applications in environmentally friendly cooling systems, compact and improved efficiency refrigeration<sup>1-9</sup>. We talk about electrocaloric effect (ECE) when an electric field applied in a higher entropy phase (usually that occur at higher temperature) of a material, reduces the entropy to the level of the lower temperature phase. Therefore, ECE brings about a reversible entropy change in the material by application of an electric field, leading to heat exchange with the environment<sup>10-14</sup>.

Solid state ECE materials typically either have high dielectric permittivity or have switchable macroscopic polarization (ferroelectric), which provide strong coupling to applied electric fields. In case of a material with paraelectric (P) – ferroelectric (F) phase sequence on cooling, the electric field aligns the molecular dipoles toward the field corresponding to a ferroelectric phase, thus reducing the entropy to the level of the F phase.

In ECE materials reversible isothermal entropy changes  $\Delta S = \int_{E_1}^{E_2} \left( \frac{\partial D}{\partial T} \right)_E dE$  and adiabatic temperature change  $\Delta T \approx - \int_{E_1}^{E_2} \frac{T}{\rho C_E} \left( \frac{\partial D}{\partial T} \right)_E dE$  are induced when an electric field changes between  $E_1$  and  $E_2$ .<sup>15</sup> In these equations  $T$  is the temperature in Kelvin scale,  $\rho$  is the mass density,  $C_E$  is the specific heat and  $\partial D / \partial T$  is the pyroelectric coefficient. For dielectric materials  $D = \epsilon_o \epsilon_r E$ , where  $\epsilon_o = 8.85 \times 10^{-12} \frac{C}{Vm}$  the permittivity of the vacuum, and  $\epsilon_r$  is the relative dielectric permittivity of the material. In case of a non-adiabatic system, the difference between the electric field  $E$  induced and the zero field paraelectric-ferroelectric transition temperatures  $\Delta T = T_{P-F}(E) - T_{P-F}(0)$  can also be called ECE induced temperature change, although the actual temperature may not change considerably in absence of a Joule heat.

In ferroelectric materials with spontaneous polarization  $P_o$ ,  $D = P_o + \epsilon_o \epsilon_r E$ . EC effects are characterized either by the EC responsivity  $\frac{\Delta T}{E}$  (Km/V), the specific isothermal entropy change  $\Delta s = \frac{\Delta S}{m}$  (J/(kg K)), and the product of the adiabatic temperature change and specific isothermal entropy change  $\Delta T \Delta s \left( \frac{J}{kg} \right)$ . Among organic solid EC materials typical values are:  $\frac{\Delta T}{E} \leq 10^{-7} \frac{Km}{V}$ ,

$\Delta s \sim 60 \frac{J}{kgK}$  and  $\Delta T \Delta s < 1 kJ/kg$ .<sup>10</sup> The largest  $\Delta T \Delta s = 2.15 kJ/kg$  values were observed in relaxor ferroelectric  $Pb_{0.8}Ba_{0.2}ZrO_3$  (PBZ) thin films<sup>16</sup>, high energy electron irradiated polyvinylidene fluoride-trifluoroethylene relaxor copolymer and in the La-doped  $PbZrTiO_3$  relaxor ceramic thin films<sup>17</sup>.

Liquid crystals (LCs) known in displays, are anisotropic dielectric fluids where orientation of the anisotropic molecules can be easily controlled by wide range of voltages with long operation life, thus making promising for large ECE. Indeed, large ECE have been observed in LCs with large dielectric anisotropy near the isotropic (I) – nematic (N)<sup>18–20</sup>, isotropic – smectic<sup>21–23</sup> and in transition to ferroelectric chiral smectic (SmC\*) phases<sup>24</sup>. At the I-N transition  $\Delta T \Delta s \sim 100 J/kg$ <sup>18</sup> was found, although they require up to  $90 V/\mu m$  fields to reach less than  $1 mC/m^2$  induced polarization<sup>18</sup>. In the transition to the SmA or SmC\* phases the EC responsivity values were  $\frac{\Delta T}{E} \leq 10^{-7} Km/V$  with typically  $\Delta T < 1 K$  and  $E > 10 V/\mu m$ . ECE in liquid crystals recently has been reviewed by Klemencic et al.<sup>25</sup>

Recently, an extraordinary new state of matter, ferroelectric nematic liquid crystals (FNLC) has been discovered<sup>26–33</sup>. Fluid FNLCs exhibit large  $>1 nC/N$  piezoelectric coupling constant<sup>34</sup> and  $\sim 50 mC/m^2$  spontaneous electric polarization that is switchable well below  $1 V/\mu m$  field<sup>30,33</sup>. Szydłowska et al.<sup>35</sup> have studied an FNLC material with isotropic – nematic (N) – ferroelectric nematic (N<sub>F</sub>) transition and found that the N-N<sub>F</sub> transition temperature can be shifted by about  $20 ^\circ C$  under  $10 V/\mu m$  DC electric fields corresponding to EC responsivity of  $\sim 2 \times 10^{-6} \frac{Km}{V}$ . Unfortunately, other characteristics of ECE were not studied and no  $\Delta s$  and  $\Delta T \Delta s$  values were reported.

Here we describe study of ECE in a newly synthesized FNLC material, PN03155 at the direct isotropic to ferroelectric nematic phase transition. The synthesis with molecular structure, the chemical characterization, the experimental methods, DSC scans and Polarized Optical Microscopy (POM) textures are described in Figure S1, Figure S2-S5, Figure S6, Figure S7 and Figure S8, respectively of the Supporting Information (SI). According to DSC, the material has a direct isotropic to ferroelectric nematic (N<sub>F</sub>) phase (corresponding to a paraelectric (P) – ferroelectric (F) transition described above) on cooling at  $69.3 ^\circ C$  that persists to room temperature. The I-N<sub>F</sub> transition is of first order; therefore, the isotropic phase can be overcooled

by  $\delta T$  and the transition happens via nucleation of  $N_F$  droplets in the isotropic phase and the transition takes  $\leq \delta T$  temperature range to be completed. In repeated measurements with the same cooling rates, the first  $N_F$  droplets consistently (within 0.1 °C) appeared at the same temperature, but there were 0.1-0.3 °C range differences for the completion of the transition. This is likely because the nucleation also depends on mechanical and noise. In spite of the competing Joule heat due to the relatively large ionic content of PN03155, we find large EC effect at unusually low ( $\sim 1 \text{ V}/\mu\text{m}$ ) fields.

## II. Results and Discussion

The FNLC material PN03155 was filled in  $d \approx 10 \mu\text{m}$  thick cells in which the glass substrates were coated with unidirectionally rubbed polyimide PI2555 that promotes planar alignment (average molecular axis parallel to the substrates) along the rubbing direction. Polarized Optical Microscopy (POM) images of cells are shown in Figure 1 at 72°C, where the first  $N_F$  droplets appear on cooling from the isotropic phase. Note, this means more than 2 °C higher transition temperature than what DSC shows likely due to the much slower cooling in POM studies than during DSC. Left column Figure 1(a,c,e) shows textures when no field is applied, while the right column Figure 1(b,d,f) shows textures when a field is applied on the LC.

The top row, Figure 1(a,b) represents textures of a film with in-plane ITO electrodes separated by 0.1 mm gap. As it can be seen in Figure 1(b) where 75 V ( $E = 0.75 \text{ V}/\mu\text{m}$ ) amplitude,  $f = 40 \text{ Hz}$  sinusoidal electric field was applied in between the in-plane electrodes, the material fully transitions from the isotropic to the  $N_F$  phase. This means the energy barrier of the field helps overcoming is the specific enthalpy change of  $4.4 \frac{\text{J}}{\text{g}}$  seen in DSC scans (see Figure S7). Importantly, as long as the Joule heat arising due to the finite conductivity of the material can be neglected, the sample temperature does not change, but only the field-induced phase transition temperature  $\Delta T = T_{I-N_F}(E) - T_{I-N_F}(0)$  is increasing, which means it can be considered as an electrocaloric (EC) effect. The existence of EC effect is further evidenced by the textural changes under  $E = 0.8 \text{ V}/\mu\text{m}$ ,  $f = 100 \text{ Hz}$  sinusoidal electric field applied between indium tin oxide (ITO) coated glass substrates. As seen in Figure 1 (c,d), the area of the birefringent  $N_F$  domains increases upon applying the field, although, in contrast to the in-plane field, the  $N_F$  phase still does not fill the entire area.

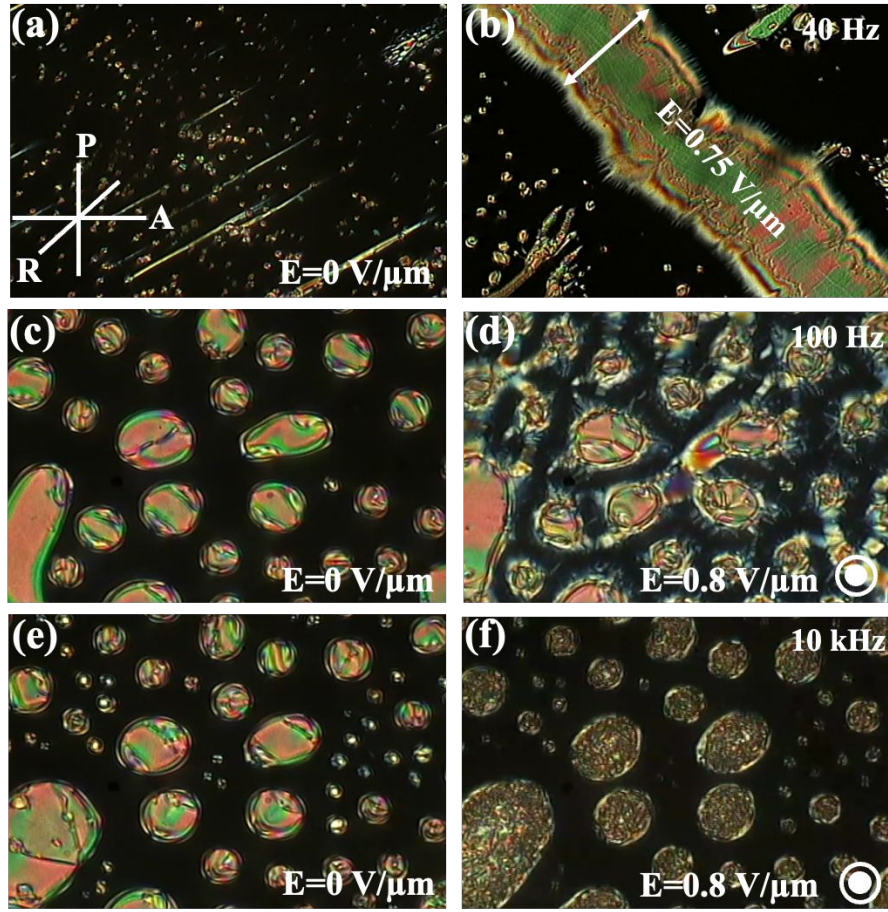


*Figure 1: Polarized Optical Microscopy (POM) images of 10  $\mu\text{m}$  thick sandwich cells with in-plane (a,b) and between planes (c-f) field geometries at 72  $^{\circ}\text{C}$ . Left column (a,c,e): No field applied; right column (b):  $E=0.75 \text{ V}/\mu\text{m}$ ,  $f=40 \text{ Hz}$  sinusoidal electric field applied in between in-plane electrodes separated by 0.1 mm gap; (d):  $E=0.8 \text{ V}/\mu\text{m}$ ,  $f=100 \text{ Hz}$  sinusoidal electric field applied in between indium tin oxide (ITO) coated glass substrates; (f):  $E=0.8 \text{ V}/\mu\text{m}$ ,  $f=10 \text{ kHz}$  sinusoidal electric field applied in between indium tin oxide (ITO) coated glass substrates.*

We have qualitatively tested that there are no significant differences in the responses below a frequency  $f \sim 200 \text{ Hz}$  where  $f < 1/\tau \sim 1/0.005 \text{ s}$ . This is because in the applied electric field range of  $0.5 \frac{\text{V}}{\mu\text{m}} < E < 1 \frac{\text{V}}{\mu\text{m}}$ , the switching time of the polarization is  $\tau < 5 \text{ ms}$ . For this reason, the difference between Figure 1(b) and Figure 1(d) is likely due to the appearance of the depolarization field  $E_{\text{dep}} = -\frac{P_o}{\epsilon_o \epsilon}$ , that acts against the applied field. The difference between the ITO coated glass substrates under  $E = 0.8 \frac{\text{V}}{\mu\text{m}}$  fields at 100 Hz seen in Figure 1(d) and that at 10 kHz shown in Figure 1(f), however is due to the large difference in the applied frequency. Namely, while at

100 Hz the polarization can follow the field, at 10 kHz it cannot be switched, i.e., the effect of the polarization disappears. Consequently, the size of the birefringence domains does not grow under such field, but only the alignment of the  $N_F$  domains change, since the material only has dielectric interaction with the 10 kHz field. This also shows that the ferroelectric polarization is needed for the EC effect under such a low electric field.

Figure 2 shows the temperature dependence of the average transmittance of a  $10\ \mu\text{m}$  cell under white light illumination at zero field between  $72\ ^\circ\text{C}$  and  $70\ ^\circ\text{C}$  using a sandwich (out-of-plane) cell. As seen in the main pane, the transmittance that is zero at  $72.2\ ^\circ\text{C}$  and reaches transmittance of  $T = 1.9$  in arbitrary units at  $72\ ^\circ\text{C}$ , increases continuously to  $T = 4.5$  at  $70\ ^\circ\text{C}$ . As shown in inset (a) of Figure 2, upon applying DC voltage  $U$  at  $72\ ^\circ\text{C}$ , the transmittance decreases to basically zero under  $U = 1.2\ \text{V}$  applied between the ITO substrates. This is due to the Joule heat  $Q = \frac{U^2}{R} \cdot t$  that in time  $t$  heats the material to the isotropic phase. Here  $R$  is the finite resistance  $R = \frac{d}{\sigma \cdot A}$  of the cell, where  $d \approx 10\ \mu\text{m}$  is the film thickness,  $A \approx 1\ \text{cm}^2$  is the area of the film, and  $\sigma$  is the electric conductivity of the material. On the other hand, when 100 Hz AC voltage is applied, the transmittance increases from  $T = 1.9$  at  $U = 0\ \text{V}$  up to  $T = 4.5$  at  $U = 12\ \text{V}$  ( $E = 1.2\frac{\text{V}}{\mu\text{m}}$ ), then it decreases to  $T = 0.6$  by  $U = 22\ \text{V}$  (see inset (b) of Figure 2). The increasing transmittance is clearly due to the ECE. Comparing the  $E = 1.2\frac{\text{V}}{\mu\text{m}}$  AC field induced highest transmittance to temperature dependent zero field transmittance, we see that it corresponds to the zero-field transmittance at  $70\ ^\circ\text{C}$ . This means  $\Delta T \approx 2\ \text{K}$  increase of the I- $N_F$  phase transition temperature under  $E = 1.2\frac{\text{V}}{\mu\text{m}}$  electric field. This increase happens in-spite of the increasing Joule heat that takes over the ECE at  $E > 1.2\frac{\text{V}}{\mu\text{m}}$ . Matching the transmittance values measured at different voltages at  $72\ ^\circ\text{C}$  with those measured at different temperatures at zero field, we can construct the  $\Delta T(E)$  function as shown in inset (c) of Figure 2.

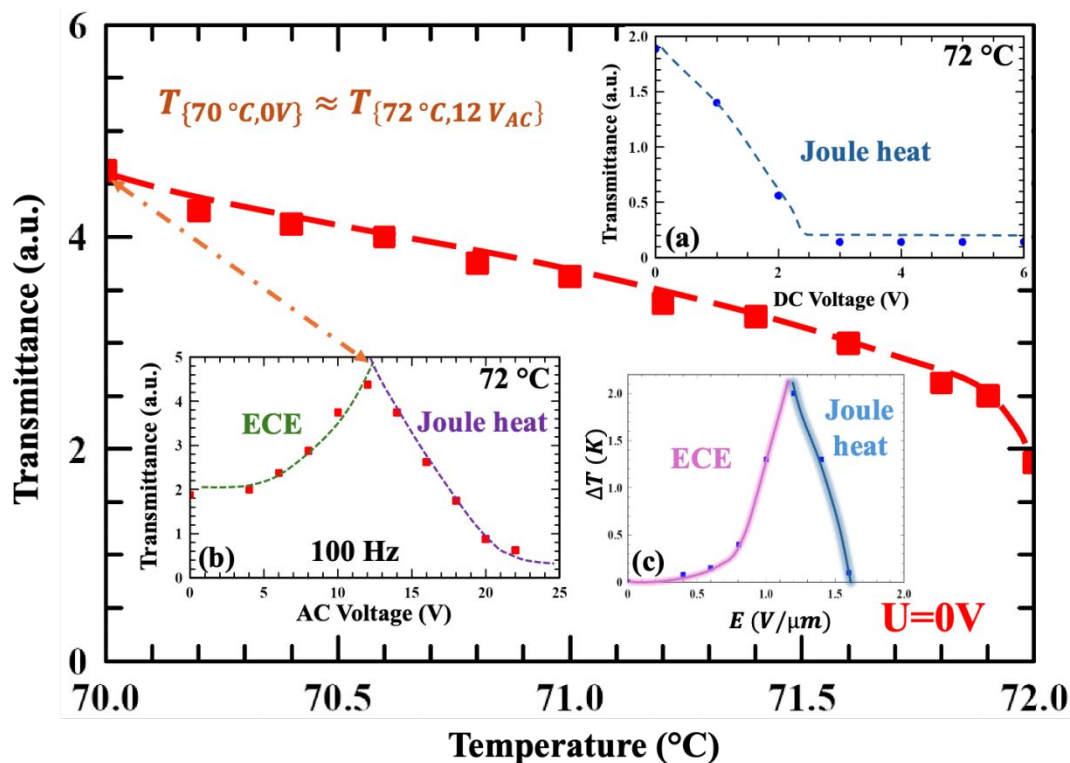


Figure 2: Temperature dependent transmittance in arbitrary units of a 10  $\mu\text{m}$  PN03155 film. Main pane: Inset (a): DC field dependence of the transmittance at 72  $^{\circ}\text{C}$ . Inset (b): 100 Hz AC field dependence of the transmittance at 72  $^{\circ}\text{C}$ . Inset (c): Construction of the 100 Hz AC electric field dependence of  $\Delta T$  by comparing the temperature dependences of the  $U=0\text{V}$  transmittance shown in main pane and of the AC voltage dependent transmittance values shown in inset (b).

The inset to Figure 3 shows the temperature dependence of the ferroelectric polarization<sup>36</sup> with values plotted against the left axis (brown triangle), and of the threshold field required to fully switch the polarization at 80 Hz triangular wave voltages plotted against the right axis (blue circle). One can see that the polarization increases from zero at 72.2  $^{\circ}\text{C}$ , where the first  $N_F$  domains appear and increases sharply reaching 2.9  $\mu\text{C}/\text{cm}^2$  value at 69  $^{\circ}\text{C}$  when the  $N_F$  domains cover the entire volume. Simultaneously, the threshold field for polarization switching increases from 0.15  $\text{V}/\mu\text{m}$  at 70  $^{\circ}\text{C}$ , up to 0.75  $\text{V}/\mu\text{m}$  at 50  $^{\circ}\text{C}$ . The plot in the main pane of Figure 3 shows the electric field dependence of the measured polarization values at several temperatures below the I- $N_F$  phase transition. One can see that in the (0.2 – 0.3)  $\text{V}/\mu\text{m}$  range the measured polarization stays close to zero at 72  $^{\circ}\text{C}$ , as the transition to the  $N_F$  phase shown in Figure 1b needed over 0.4  $\text{V}/\mu\text{m}$  field as seen in inset (b) of Figure 2. At temperatures between 64  $^{\circ}\text{C}$  and 70  $^{\circ}\text{C}$  the



polarization increases with field. We note that for  $T < 70^\circ\text{C}$ , the  $N_F$  phase is completely formed, i.e., the measurement is performed in the single-phase  $N_F$ . In contrast to measurements at  $T > 70^\circ\text{C}$ , where we induce the  $I$ - $N_F$  phase transition due to ECE, in the completely formed  $N_F$  phase we increase the polar order, thus the value of the ferroelectric polarization. This is a field-induced quenching of the thermal fluctuations. Note, the increase of the zero-field polarization toward lower temperatures as seen in the inset, is also due to the increase of the polar order (decrease of the director fluctuation). Therefore, the field-induced increase of the polar order can also be interpreted as field induced increase of the  $I$ - $N_F$  transition temperature  $\Delta T = T_{I-N_F}(E) - T_{I-N_F}(0)$  as a consequence of the ECE.

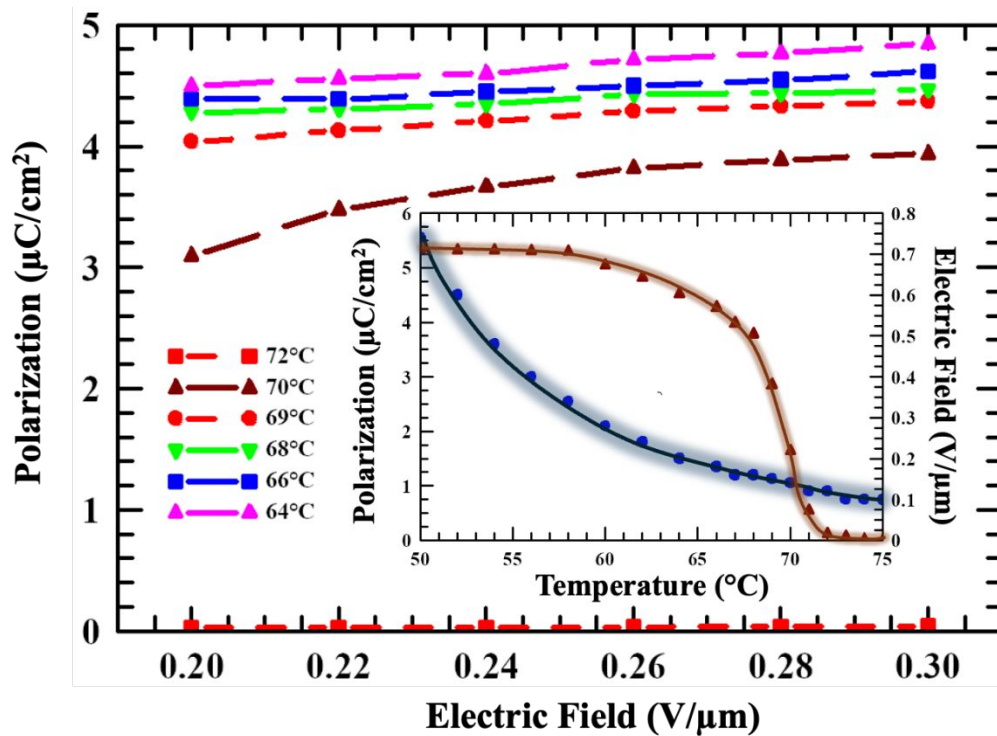


Figure 3: Electric field dependence of the measured polarization values at various temperatures. Inset: Temperature dependence of the spontaneous polarization (left axis, brown triangle) and of the threshold voltage needed for full switching (right axis, blue circle). Width of the glow represents the measurement error.

Our results presented in Figure 2 allow us to quantify the ECE of our ferroelectric nematic liquid crystal in terms of the EC responsivity  $\frac{\Delta T}{E}$  (K/V), the specific isothermal entropy change  $\Delta s = \frac{\Delta S}{m}$  (J/(kg K)), and the product of the ECE temperature change and specific isothermal entropy change

$\Delta T \Delta s \left( \frac{J}{kg} \right)$ . The observed  $\Delta T \approx 2 \text{ K}$  under  $1.2 \text{ V}/\mu\text{m}$  gives the EC responsivity to be  $\approx 1.7 \times 10^{-6} \text{ Km}/\text{V}$ , which is an order of magnitude larger than found in organic solids, N and SmA liquid crystals, and about the same as we calculated for another ferroelectric nematic LC material<sup>35</sup>. This large EC responsivity is mainly due to the extremely low field required for the switching of the ferroelectric polarization. The specific isothermal entropy change can be calculated from the specific transition enthalpy  $H \approx 4.4 \frac{J}{g} = T \Delta s$ , giving  $\Delta s \approx \frac{4400 \text{ J/kg}}{(273+72)K} \approx 13 \text{ J/(kg} \cdot \text{K)}$ , and  $\Delta T \Delta s \approx 26 \text{ J/kg}$ . Although the obtained  $\Delta T \Delta s$  value is  $\sim 3$  times smaller than found in dielectric LCs<sup>18</sup> at the  $I - N$  transition, its required field is over 100 times smaller.

Finally, we show that the experimentally observed EC responsivity corresponds to a value that we can calculate from the electric analogy of the Clausius-Clapeyron equation that relates the pressure dependent slope of the melting temperature  $dT/dp$ , the specific enthalpy  $H$  (obtained from DSC measurement shown in Figure S7) and the specific volume change  $\Delta v$  at the phase transition temperature  $T$  as  $\frac{dT}{dp} = \frac{T \cdot \Delta v}{H}$ . Replacing the specific work of the pressure  $dp \cdot \Delta v$  with the specific electrical energy  $(PE + \frac{1}{2} \epsilon_o \epsilon E^2)/\rho$ , where the first term is the ferroelectric, and the second term is the dielectric specific energy density, and  $\rho$  is the mass density, we arrive to the equation,  $\frac{\Delta T}{T} = \frac{PE + \frac{1}{2} \epsilon_o \epsilon E^2}{\rho \Delta H}$ . Taking the polarization value  $P \approx 0.03 \text{ C/m}^2$  (see inset to Figure 3) when the ferroelectric nematic phase is completely formed at  $T \approx 70^\circ\text{C} \approx 343 \text{ K}$ , the mass density of  $\rho \approx 1.3 \cdot 10^3 \text{ kg/m}^3$ ;  $H \approx 4.4 \cdot 10^3 \text{ J/kg}$  and electric field  $E = 1.2 \times 10^6 \text{ V/m}$ , furthermore neglecting the dielectric term, one obtains  $\Delta T \approx 2.1 \text{ K}$ . This agrees well with the experimentally observed  $\Delta T \approx 2.0 \text{ K}$ . We note that in the isotropic phase one may expect only dielectric coupling with the electric field. To cause the observed  $\Delta T \sim 2^\circ\text{C}$  at  $E = 1.2 \text{ V}/\mu\text{m}$ , that coupling would require  $\epsilon \sim 5 \cdot 10^3$  dielectric constant. This value is clearly too large for the isotropic phase. For this reason, we think the polar interaction we assumed is valid, because in the temperature range the ECE was observed, the material is overcooled, and the ferroelectric phase is thermodynamically more stable.

To summarize, we have described and quantitatively characterized the electrocaloric effect of a newly synthesized ferroelectric nematic liquid crystal compound (PN03155) at the isotropic ferroelectric nematic (I- $N_F$ ) phase transition. While for DC field the Joule heat completely

suppresses the ECE, at  $f \geq 40$  Hz harmonic AC fields the ECE dominates below  $1 \text{ V}/\mu\text{m}$  field with a  $\sim 1.7 \times 10^{-6} \text{ Km}/\text{V}$  EC responsivity. Although the product of the adiabatic temperature change and specific isothermal entropy change,  $\Delta T \Delta s \approx 26 \text{ J}/\text{kg}$  is three times smaller than found in dielectric LCs<sup>18</sup> at the  $I - N$  transition, the required field is over 100 times smaller. EC effect under such low fields is a unique property of ferroelectric nematic liquid crystals. Although one may argue that AC fields are useless as there is no time for heat to flow after applying and removing the field, in our case, both polarity of the field induces the shift in the phase transition as long as the frequency of the field is low enough to fully switch the polarization. Therefore, the heat flow is removed upon turning off the field and not during polarity reversal. Additionally, the obtained  $\Delta T \Delta s$  values can be increased considerably by reducing the ionic content, thus suppressing the Joule heat.

### III. Acknowledgement

This work was financially supported by US National Science Foundation grant DMR-2210083. We thank for useful discussions with Professors S. Sprunt and J. Gleeson at Kent State University.

### IV. References

- 1 J. Z. Hao, F. X. Hu, Z. B. Yu, F. R. Shen, H. B. Zhou, Y. H. Gao, K. M. Qiao, J. Li, C. Zhang, W. H. Liang, J. Wang, J. He, J. R. Sun and B. G. Shen, *Chinese Physics B*, 2020, **29**, 047504.
- 2 M. M. Vopson, *J Phys D Appl Phys*, 2013, **46**, 345304.
- 3 I. N. Flerov, E. A. Mikhaleva, M. V. Gorev and A. V. Kartashev, *Physics of the Solid State*, 2015, **57**, 429–441.
- 4 A. Gschneidner, V. K. Pecharsky and A. O. Tsokol, *Reports on Progress in Physics*, 2005, **68**, 1479–1539.
- 5 A. S. Mischenko, Q. Zhang, J. F. Scott, R. W. Whatmore and N. D. Mathur, *Science (1979)*, 2006, **311**, 1270–1271.
- 6 L. Mañosa, D. González-Alonso, A. Planes, M. Barrio, J. L. Tamarit, I. S. Titov, M. Acet, A. Bhattacharyya and S. Majumdar, *Nat Commun*, 2011, **2**, 595.

- 7 M. S. Gruzdev, V. V. Korolev, A. G. Ramazanova, U. V. Chervonova and O. V. Balmasova, *Liq Cryst*, 2018, **45**, 907–911.
- 8 G. Skačej, *Liq Cryst*, 2018, **45**, 1964–1969.
- 9 J. Cui, Y. Wu, J. Muehlbauer, Y. Hwang, R. Radermacher, S. Fackler, M. Wuttig and I. Takeuchi, *Appl Phys Lett*, 2012, **101**, 073904.
- 10 Z. Kutnjak, B. Rožič and R. Pirc, in *Wiley Encyclopedia of Electrical and Electronics Engineering*, Wiley, 2015, pp. 1–19.
- 11 R. I. Epstein and K. J. Malloy, *J Appl Phys*, 2009, **106**, 064509.
- 12 Y. S. Ju, *J Electron Packag*, 2010, **132**, 041004.
- 13 H. Gu, X. Qian, X. Li, B. Craven, W. Zhu, A. Cheng, S. C. Yao and Q. M. Zhang, *Appl Phys Lett*, 2013, **102**, 122904.
- 14 C. Aprea, A. Greco, A. Maiorino and C. Masselli, in *Journal of Physics: Conference Series*, Institute of Physics Publishing, 2017, vol. 796, p. 012019.
- 15 Bret Neese, Baojin Chu, Sheng-Guo Lu, Yong Wang, E. Furman and Q.M. Zhang, *Science (1979)*, 2008, **321**, 821–823.
- 16 B. Peng, H. Fan and Q. Zhang, *Adv Funct Mater*, 2013, **23**, 2987–2992.
- 17 S. G. Lu, B. Rožič, Q. M. Zhang, Z. Kutnjak, X. Li, E. Furman, L. J. Gorny, M. Lin, B. Malič, M. Kosec, R. Blinc and R. Pirc, *Appl Phys Lett*, 2010, **97**, 162904.
- 18 X. S. Qian, S. G. Lu, X. Li, H. Gu, L. C. Chien and Q. Zhang, *Adv Funct Mater*, 2013, **23**, 2894–2898.
- 19 I. Lelidis and G. Durand, *Phys Rev Lett*, 1996, **76**, 1868–1871.
- 20 X.-S. Qian, S. G. Lu, X. Li, H. Gu, L.-C. Chien, Q. M. Zhang, L.-C. Chien, Q. M. Zhang, L.-C. Chien and Q. M. Zhang, *MRS Proceedings*, 2013, **1543**, 13–20.
- 21 M. Trèek, M. Lavriè, G. Cordoyiannis, B. Zalar, B. Rožič, S. Kralj, V. Tzitzios, G. Nounesis and Z. Kutnjak, *Philosophical Transactions of the Royal Society A*, 2016, **374**, 20150301.

- 22 D. Črešnar, N. Derets, M. Trček, G. Skačej, A. Rešetič, M. Lavrič, V. Domenici, B. Zalar, S. Kralj, Z. Kutnjak and B. Rožič, *J Phys Energy*, 2023, **5**, 045004.
- 23 E. Klemenčič, M. Trček, Z. Kutnjak and S. Kralj, *Sci Rep*, 2019, **9**, 1721.
- 24 E. Bsaibess, A. Hadj Sahraoui, Y. Boussoualem, M. Soueidan, B. Duponchel, D. P. Singh, B. Nsouli, A. Daoudi and S. Longuemart, *Liq Cryst*, 2019, **46**, 1517–1526.
- 25 E. Klemencic, M. Trecek, Z. Kutnjak and S. Kralj, in *The Electrocaloric Effect*, 2023, pp. 205–223.
- 26 R. J. Mandle, S. J. Cowling and J. W. Goodby, *Physical Chemistry Chemical Physics*, 2017, **19**, 11429–11435.
- 27 A. Mertelj, L. Cmok, N. Sebastián, R. J. Mandle, R. R. Parker, A. C. Whitwood, J. W. Goodby and M. Čopič, *Phys Rev X*, 2018, **8**, 041025.
- 28 N. Sebastián, L. Cmok, R. J. Mandle, M. R. De La Fuente, I. Drevenšek Olenik, M. Čopič and A. Mertelj, *Phys Rev Lett*, 2020, **124**, 037801.
- 29 R. J. Mandle, N. Sebastián, J. Martinez-Perdiguero and A. Mertelj, *Nat Commun*, 2021, **12**, 4962.
- 30 H. Nishikawa, K. Shiroshita, H. Higuchi, Y. Okumura, Y. Haseba, S. Yamamoto, K. Sago and H. Kikuchi, *Advanced Materials*, 2017, **29**, 1702354.
- 31 R. J. Mandle, S. J. Cowling and J. W. Goodby, *Chemistry - A European Journal*, 2017, **23**, 14554–14562.
- 32 N. Sebastián, M. Čopič and A. Mertelj, *Phys Rev E*, 2022, **106**, 021001.
- 33 X. Chen, E. Korblova, D. Dong, X. Wei, R. Shao, L. Radzihovsky, M. A. Glaser, J. E. MacLennan, D. Bedrov, D. M. Walba, N. A. Clark, N. L. Abbott, P. Palfy-Muhoray, P. Pieranski, A. contributions, N. designed research, N. performed research and N. analyzed data, *Proc Natl Acad Sci USA*, 2020, **117**, 14021–14031.
- 34 M. T. Máthé, M. S. H. Himel, A. Adaka, J. T. Gleeson, S. Sprunt, P. Salamon and A. Jákli, *Adv Funct Mater*, 2024, 2314158.

- 35 J. Szydłowska, P. Majewski, M. Čepič, N. Vaupotič, P. Rybak, C. T. Imrie, R. Walker, E. Cruickshank, J. M. D. Storey, P. Damian and E. Gorecka, *Phys Rev Lett*, 2023, **130**, 216802.
- 36 Keita Miyasato, Shigeharu Abe, Hideo Takezoe, Atsuo Fukuda and Eiichi Kuze, *Jpn J Appl Phys*, 1983, **22**, L661–L663.

Dear Editor,

The raw data of our manuscript entitled “Low Field Electrocaloric Effect at Isotropic - Ferroelectric Nematic Liquid Transition” by Adaka et al will be made available by the corresponding author upon reasonable request.

Sincerely Yours,

Antal I. Jákli,

Professor, Department of Physics

Director of Materials Science Graduate Program

Advanced Materials and Liquid Crystal Institute,

Kent State University, Kent, OH 44242, USA

E-mail: [ajakli@kent.edu](mailto:ajakli@kent.edu);

Tel: +1 330 672 4886

Web: <http://media.kent.edu/~ajakli/>